J. Biochem. 121, 787-797 (1997)

Linear Polymerization Caused by the Defective Folding of a Non-Inhibitory Serpin Ovalbumin[1]

Nobuaki Shirai, Fumito Tani,[2] Takahiko Higasa, and Kyoden Yasumoto

Research Institute for Food Science, Kyoto University, Uji, Kyoto 611

Received for publication, December 16, 1996

Polymerization caused by defective folding of heat-denatured ovalbumin was examined. A compactly misfolded ovalbumin that was produced by cooling heat-denatured protein rapidly tended to aggregate in the presence of salt. Two different forms of aggregates were observed as the concentration of salt was varied: a linear polymer at a physiological concentration and a massive agglomerate at a higher concentration. Salt-induced polymerization depended on the species of anion and the order of effectiveness followed the lyotropic series of Hofmeister. Defective folding of heat-denatured ovalbumin induced the exposure of cysteine residues in sequences located in the interior of the native protein. The misfolded ovalbumin, but not the native protein, bound to bovine BiP and stimulated its ATPase activity with the K_m of 64 μM and the V_{max} of 0.5 nmol/min per milligram. Measurement of surface plasmon resonance revealed that only the misfolded ovalbumin was recognized with the K_d of 4.12×10^{-8} M by the Fab fragment of a monoclonal antibody raised against hen ovalbumin, and its epitope was determined to be a hydrophobic segment in the β-strand of central sheet A. Transmission electron microscopy showed that the linear polymerization was inhibited by the addition of bovine BiP and the Fab fragment. These results demonstrated that the compactly misfolded ovalbumin polymerized through hydrophobic interaction occurring among the areas exposed as a result of defective folding of the heat-denatured protein. Exposure of the region of, or adjacent to, the central β-sheet A was required for axial contact among the misfolded molecules, suggesting that this process may be explained by reference to the mechanism proposed for loop-sheet polymerization in the Z type variant of a serpin α_1-antitrypsin.

Key words: BiP, defective folding, linear polymerization, ovalbumin, serpin superfamily.

Aggregation retards correct folding of unfolded protein molecules. Unfolded polypeptides are committed either to refold correctly to the native structure or to aggregate to a dysfunctional product. Small proteins such as apomyoglobin and α-lactalbumin tend predominantly to refold rapidly and spontaneously (*1, 2*). By contrast, large proteins are likely to refold slowly and inefficiently because of their more complicated structures. Moreover, as a polypeptide chain increases in length, there is an increased probability of genetic mutations so that a large protein is more vulnerable to changes in structural organization during its folding process (*3*).

Mutations of a serine protease inhibitor (serpin) trigger a defective folding of the variants that leads to the polymerization of misfolded proteins, and this is the cause of a diverse range of diseases (*4*). Human α_1-antitrypsin, an archetypal member of the serpin superfamily, is synthesized in hepatocytes of the liver (*5, 6*) and secreted into the circulation as a component of the plasma (*5*). Its physiological role is the protection of lung elastin fibers from proteolytic attack by neutrophil elastase (*7*). Some genetic variants of this inhibitor, for example the Z type variant (*8, 9*), cause aggregation of the protein in the endoplasmic reticulum of hepatocytes, thereby inducing liver damage, plasma deficiency of the inhibitor and ultimately, lung emphysema (*4, 10-12*). Recently Yu and colleagues demonstrated clearly that, unlike wild-type α_1-antitrypsin, which folds in minutes, the folding of Z type variant of α_1-antitrypsin is extremely slow (*13*) and this is a cause of aggregation (*14*). As the mechanism for spontaneous aggregation of the Z variant, a persuasive model of loop-sheet polymerization has been proposed, in which the mobile reactive-center loop of one molecule is inserted into the central β-sheet of another (*15-18*).

Ovalbumin, a globular protein of chicken egg white with a molecular size of 45 kDa, is a member of the serpin superfamily, along with α_1-antitrypsin (*19*). Ovalbumin shows no inhibitory activity (*20, 21*), despite sequence

[1] This work was supported in part by a Grant-in-Aid for Encouragement of Young Scientists (No. 07856008) to F.T. and a Grant-in-Aid for Exploratory Research (No. 08876027) to F.T. from the Ministry of Education, Science, Sports and Culture of Japan.

[2] To whom correspondence should be addressed. Tel: +81-774-38-3741, Fax: +81-774-38-3740, E-mail: tani@soya.food.kyoto-u.ac.jp

Abbreviations: BiP, immunoglobulin heavy chain binding protein; BSA, bovine serum albumin; EDC, *N*-ethyl-*N'*-((3-dimethylamino) propyl)carbodiimide hydrochloride; HPLC, high-performance liquid chromatography; IAEDANS; *N*-iodoacetyl-*N'*-(5-sulfo-1-naphthyl) ethylenediamine; NHS, *N*-hydroxysuccinimide; PAGE, polyacrylamide gel electrophoresis; PEI, polyethyleneimine; PMSF, phenylmethylsulfonyl fluoride; PVDF, polyvinylidene difluoride; RU, resonance unit; SDS, sodium dodecyl sulfate; TEM, transmission electron microscopy; TLC, thin layer chromatography.

homology of about 30% with antitrypsin, but acts as a substrate of elastase (*22*), and hence is classified as a non-inhibitory serpin. The crystal structure of native ovalbumin (*23*) indicates that a five-stranded β-sheet (β-sheet A) runs parallel to the long axis of the molecule and that an α-helix protrudes as a loop that forms the reactive center (see also Fig. 10A in "DISCUSSION"). Native ovalbumin has a disulfide bond in a solvent-accessible environment and four cysteine residues with free sulfhydryl groups within the intramolecular hydrophobic core (*23*). Considering that ovalbumin has both thiol and disulfide moieties, it is considered that non-native disulfide pairings are formed owing to a rapid thiol-disulfide exchange under non-reducing and denaturing conditions (*24*), and that they disturb correct folding of chemically denatured ovalbumin (*25*). Recently we demonstrated that rapid cooling caused a defective folding of heat-denatured ovalbumin as a result of non-native disulfide pairings, and that the rapidly cooled ovalbumin assumed a compactly misfolded conformation with molten globule-like characteristics as a folding intermediate (Tani, F. *et al.*, submitted for publication). This compactly misfolded ovalbumin was shown to remain monomeric at a low ionic strength. On the other hand, when heated at 80°C in the presence of salt, ovalbumin produces a highly ordered linear polymer (*26*), as does α_1-antitrypsin (*4, 17*). Ovalbumin molecules in a chain polymer were found to adopt molten globule-like structures (*27*).

In the present study, we examined the details of molecular interaction for polymerization of ovalbumin by manipulating the ionic strength of the medium that contains the compactly misfolded protein. We also discuss the mechanism of linear polymerization of misfolded ovalbumin in the light of defective folding and polymerization of serpins, that are associated with diverse diseases.

MATERIALS AND METHODS

Materials—Ovalbumin was purified from the egg white of newly laid hens' eggs by crystallization in a solution of ammonium sulfate and was recrystallized five times (*28*). A monoclonal antibody was raised against hen ovalbumin that had been denatured by γ-ray irradiation according to a conventional method by Koseki *et al.* in our laboratory (manuscript in preparation). A sequence-specific Fab fragment was prepared by the cleavage of this monoclonal antibody with papain. For detection of bovine BiP, a monoclonal antibody, which recognizes the consensus sequence of heat shock protein 70 family (*29*), was obtained from Affinity BioReagents (Neshanic Station, NJ, USA). A polyclonal antibody raised against hen ovalbumin and alkaline phosphatase-conjugated goat anti-rat IgG antibody with no cross-reactivity to mouse IgG were obtained from Organon Teknika (Durham, NC, USA). Protein A Sepharose was purchased from Pharmacia (Uppsala, Sweden). Nitro blue tetrazolium and 5-bromo-4-chloro-3-indolyl phosphate were purchased from Promega (Madison, WI, USA), and papain, trypsin (type III), chymotrypsin (type II), and BSA (Fraction V) from Sigma Chemical (St. Louis, MO, USA). *Achromobacter* protease I [EC 3.4.21.50] was obtained from Wako Pure Chemical Industries (Osaka). IAEDANS was purchased from Aldrich Chemical (Milwaukee, WI, USA). Iodoacetoamide, urea of specially prepared reagent grade and other chemicals of guaranteed grade were obtained from Nacalai Tesque (Kyoto).

Salt-Induced Polymerization of Misfolded Ovalbumin—A solution of ovalbumin at 0.25 mg/ml, containing 0.01 mM EDTA, was adjusted to pH 7.5 with 0.1 N NaOH and a pH meter (Toko Chemical Lab., Tokyo). After adjustment of the pH, an aliquot of the solution was heated at 80°C for 5 min in a borosilicate glass tube and cooled rapidly in an ice-water bath to obtain the compactly misfolded ovalbumin. The solution of the misfolded ovalbumin was concentrated by membrane filtration (Centriprep-30™; Amicon, Beverly, MA, USA) to a protein concentration above 2 mg/ml. To obtain samples of ovalbumin aggregates for size-exclusion chromatography, the misfolded ovalbumin was incubated at 1 mg/ml at 37°C for various periods (1, 6, and 24 h) in 10 mM Tris (pH 7.5) containing 50 mM KCl. To obtain samples for TEM observation, the protein solution was incubated at 2.8 mg/ml at 37°C for 5 h in 20 mM Hepes (pH 7.5) containing KCl at 50 mM, 150 mM, and 450 mM, or the buffer without KCl.

Size-Exclusion Chromatography—The aggregates of misfolded ovalbumin were analyzed on a column of TSKgel G3000SW$_{XL}$ (7.8 i.d.$\times$300 mm; Tosoh, Tokyo). The column was equilibrated with 20 mM potassium phosphate buffer (pH 7.5), and the samples were eluted with the same buffer at a flow rate of 0.5 ml/min. The amount of ovalbumin applied to the column was 2.5 μg.

Precipitation and Perpendicular Light Scattering—For the precipitation experiment, the solution of misfolded ovalbumin was incubated at 1 mg/ml at 37°C in the presence of 10 mM Hepes (pH 7.5) containing different anions. After the incubation for 30 min, the samples were placed in an ice-water bath for 5 min, and centrifuged for 10 min at 10,000$\times g$. The absorbance of the supernatant obtained was measured at 280 nm.

For the light-scattering experiment, 20 mM Hepes (pH 7.5) containing a variety of anions at 300 mM was placed in a cuvette that was thermostatically maintained at 37°C. Polymerization was initiated by the addition to the cuvette of equal volumes of the misfolded ovalbumin solution to give a final concentration of 1 mg/ml. Perpendicular light scattering was monitored for 1 h at 320 nm in a fluorometer (F-3000; Hitachi, Tokyo).

Identification of Exposed Sulfhydryl Groups—A solution of Tris buffer containing IAEDANS was added to an aliquot of ovalbumin solution to give a final concentration of 0.13 mg/ml in 50 mM Tris (pH 8.2), 1 mM EDTA, and 10 mM IAEDANS, for labeling of the exposed free sulfhydryl groups. After incubation at 37°C for 15 min, the protein was precipitated with a mixture of cold acetone and 1 N HCl (98 : 2, v/v), washed three times with a mixture of cold acetone, 1 N HCl, and H_2O (98 : 2 : 10, v/v), dissolved in buffer [50 mM Tris (pH 8.2), 1 mM EDTA] that contained 9 M urea to give a protein concentration of 0.25 mg/ml, and then fully reduced by incubation with 5 mM DTT at 37°C for 30 min. The reduced protein was mixed with 160 mM iodoacetamide, and alkylation of protein sulfhydryl groups was achieved by incubation at 37°C for 10 min. As a standard sample, ovalbumin was fully reduced and unfolded at 37°C for 30 min in the presence of Tris buffer containing 9 M urea and 5 mM DTT. After the incubation, disulfide-reduced ovalbumin was labeled at 37°C for 15 min with 15 mM IAEDANS. The labeled proteins were pre-

cipitated with acetone-HCl, washed as described above, and extensively digested by two-step proteolysis. Procedures for two-step proteolysis and separation of the peptides were those developed by Tatsumi *et al.* (*24*). The percentage of exposed cysteine residues was estimated in terms of the ratio of areas of the peaks showing fluorescent material in a sample to those of the corresponding peaks in the standard.

Purification of Bovine BiP—Fresh bovine liver was homogenized in buffer A [20 mM Tris (pH 7.5), 1 mM EDTA, 0.5 mM PMSF, and 0.25 M sucrose] with a Potter-Elvehjem homogenizer. The homogenate was centrifuged for 10 min at 750 × *g* and then for 10 min at 7,000 × *g*. The microsome fraction was isolated from the obtained supernatant by sedimentation for 60 min at 100,000 × *g* through a 20% sucrose cushion in buffer A. The resultant pellet was collected as the crude microsome fraction and suspended in buffer A. BiP was purified from the crude microsome fraction according to the method of Flynn *et al.* (*30*). Free ATP as well as ATP bound to bovine BiP was removed by precipitation of the protein in saturated $(NH_4)_2SO_4$ solution containing 10 mM EDTA. For use, the precipitate was dissolved in and dialyzed against 20 mM Tris (pH 7.5).

Assays of Polypeptide Binding to BiP—For analysis of polypeptide binding, 3.9 μg of purified bovine BiP (50 pmol) was incubated at 37°C for 30 min with 2.3 μg of either the misfolded ovalbumin or the native protein (50 pmol) in a final volume of 20 μl of 20 mM Tris (pH 7.5) containing 140 mM KCl and 3 mM $MgCl_2$. The BiP-ovalbumin complexes were separated from free BiP by the addition of protein A Sepharose beads (20 μl) that had been preloaded with rabbit polyclonal antibody against hen ovalbumin. After mixing at 37°C for 30 min, the Sepharose beads bearing the bound complexes were recovered by centrifugation at 3,000 × *g*, washed three times with 0.5 ml of the reaction buffer, suspended in SDS-PAGE sample buffer [62.5 mM Tris (pH 7.0), 1% SDS, 10% glycerol, 20 mM 2-mercaptoethanol], and treated in a boiling water bath for 5 min. An aliquot of the supernatant was electrophoresed on 7.5% SDS-polyacrylamide gel according to the standard method used by Laemmli (*31*) and proteins were electroblotted onto a PVDF membrane (Bio-Rad Lab.; Hercules, CA, USA) in the same way as described by Hirano (*32*). BiP was probed with rat monoclonal antibody to a peptide containing the sequence conserved in heat shock proteins and the blot was developed with alkaline phosphatase-conjugated goat antibody against rat IgG in a mixture of nitro blue tetrazolium and 5-bromo-4-chloro-3-indolyl phosphate.

ATPase Assays—ATPase activity was measured by the method of Shlomai and Kornberg (*33*) using TLC on PEI cellulose (Macherey-Nägel; Düren, Germany) to separate nucleotides. Purified BiP (1 μg) was incubated at 37°C for 20 min with various concentrations of ovalbumin in a volume of 20 μl of the buffer [20 mM Hepes (pH 7.0), 20 mM KCl, 2 mM $MgCl_2$, and 10 mM $(NH_4)_2SO_4$] that was supplemented with 8 μM ATP containing 0.5 μCi [α-^{32}P]ATP. Stimulation of ATPase activity was assayed in the presence of ovalbumin over a concentration range from 10 μM to 0.3 mM. Aliquots of the reaction mixtures (2 μl) were spotted on PEI plates that had been prespotted with 1 μl of a mixture of nonradioactive AMP, ADP, and ATP (each 10 mM). The chromatography was developed to 15 cm in a mixture of 0.5 M LiCl and 1 M formic acid, and the plate was dried. The ATP and ADP spots were located under ultraviolet light at 254 nm. The radioactivity corresponding to each spot was quantitated with a FUJIX Bio-Imaging Analyzer BAS 2000 (Fuji Photo Film, Tokyo) and expressed as a fraction of the total recovered in each lane.

Measurement of Surface Plasmon Resonance—In the BIAcore 2000™ system (Pharmacia Biosensor AB, Uppsala, Sweden) (*34*), the Fab fragment of the monoclonal antibody raised against radiochemically denatured ovalbumin [50 μg/ml in 10 mM sodium acetate buffer (pH 5.0)] was immobilized on the dextran matrix of the sensor-chip (CM5) surface with a 1:1 mixture of NHS and EDC. The excess active groups on the dextran matrix were blocked with 1 M ethanolamine (pH 8.5) (*35*). The Fab fragment was immobilized at the concentration of 3 ng/mm². The freshly prepared ovalbumin samples were passed over the sensor surface at 25°C at a flow rate of 5 μl/min at concentrations ranging from 200 to 600 nM. The running buffer used in this experiment was 10 mM Hepes (pH 7.4) containing 150 mM NaCl, 3.4 mM EDTA, and 0.005% Tween 20. Kinetic analyses were performed with the supplemental software BIAevaluation 2.0 (Pharmacia). We calculated the association rate constant, k_{ass}, and dissociation rate constant, k_{diss}, using curve fitting to a simple two-component model of interaction (A + B = AB) for titration of the solution-phase ligand. The equilibrium dissociation constant, K_d, was determined as k_{diss}/k_{ass}.

Competition Experiment—A solution of the misfolded ovalbumin was incubated at 1 mg/ml at 37°C for 18 h with a competitor, either bovine BiP or the anti-ovalbumin Fab fragment, in 20 mM Mops (pH 7.0) buffer containing 150 mM KCl, to allow the formation of ovalbumin polymers, and was observed by using a transmission electron microscope (Hitachi H-700H; Tokyo). The amount of the competitor was half that of ovalbumin in molar ratio. Other proteins used for control experiments were BSA and the Fab fragment of the monoclonal antibody raised against transglutaminase, neither of which exhibit any reactivity with hen ovalbumin.

TEM Techniques—The protein solutions were diluted 15 to 50-fold with the same buffer as used for preparing the specimen. The specimen was placed on a carbon-coated electron microscope grid, negatively stained with 2% potassium phosphotungstate, and observed with a transmission electron microscope (Hitachi H-700H; Tokyo) operating at 100 kV.

RESULTS

Salt-Induced Polymerization of Misfolded Ovalbumin—Salt-induced polymerization of the misfolded ovalbumin was examined by size-exclusion chromatography on a column of TSKgel G3000SW$_{XL}$, which was able to separate proteins up to the molecular size of 5×10^5 kDa with high resolution. In the absence of salt (Fig. 1A), a large portion of the misfolded molecules remained in a monomeric state. By contrast, in the presence of 50 mM KCl, the molecules aggregated easily to form oligomers when incubated for 1 h (Fig. 1B). Prolonged incubation promoted aggregation of the misfolded ovalbumin, as judged from the migration of the peak corresponding to oligomers toward the position of the void volume (Fig. 1C). A large peak at the void volume

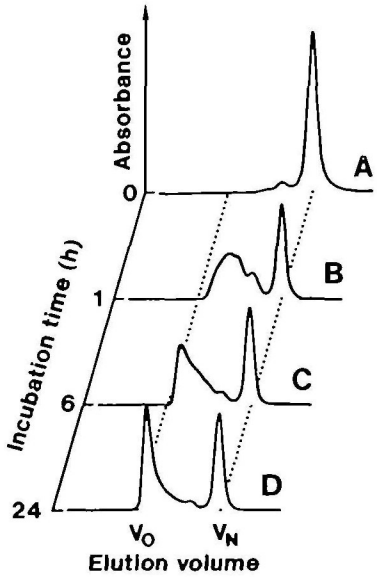

Fig. 1. **Comparison of the elution profiles of variously treated samples of ovalbumin during size-exclusion chromatography.** Ovalbumin that had been heat-denatured at 80°C for 5 min was cooled rapidly in an ice-water bath. The compactly misfolded ovalbumin was concentrated by membrane filtration (Centriprep-30™) in the absence of KCl (A). The misfolded ovalbumin solution was incubated at 1 mg/ml at 37°C in the presence of 50 mM KCl for various periods: (B) for 1 h; (C) for 6 h; (D) for 24 h. An aliquot of each ovalbumin sample was analyzed on a column of TSKgel G3000SW$_{XL}$, which was equilibrated with 20 mM potassium phosphate buffer (pH 7.5), and eluted with the same buffer at a flow rate of 0.5 ml/min. The amount of ovalbumin applied to the column was 2.5 μg. V_O and V_N indicate the void volume of blue dextran and the elution volume of native ovalbumin, respectively. Absorbance at 280 nm is in arbitrary units.

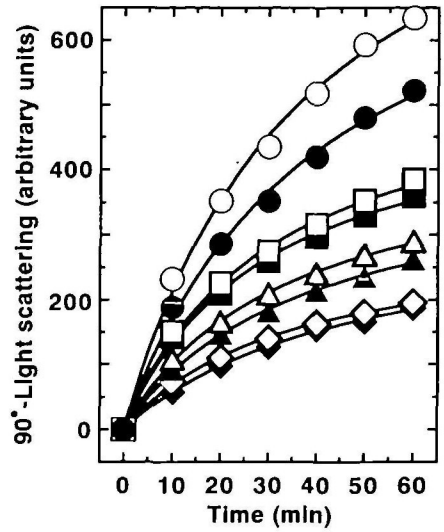

Fig. 3. **Effect of different sodium anions on the elongation of chain polymers of ovalbumin evaluated in terms of perpendicular light scattering.** The misfolded ovalbumin solution was mixed at 37°C with equal volumes of 20 mM Hepes (pH 7.5) containing a variety of anions at 300 mM to give a final concentration of 1 mg/ml. Perpendicular light scattering was monitored for 1 h at 320 nm in a fluorometer. Anions used were as follows: sulfate (open circle); phosphate (closed circle); acetate (open square); fluoride (closed square); chloride (open triangle); bromide (closed triangle); iodide (open diamond); thiocyanate (closed diamond).

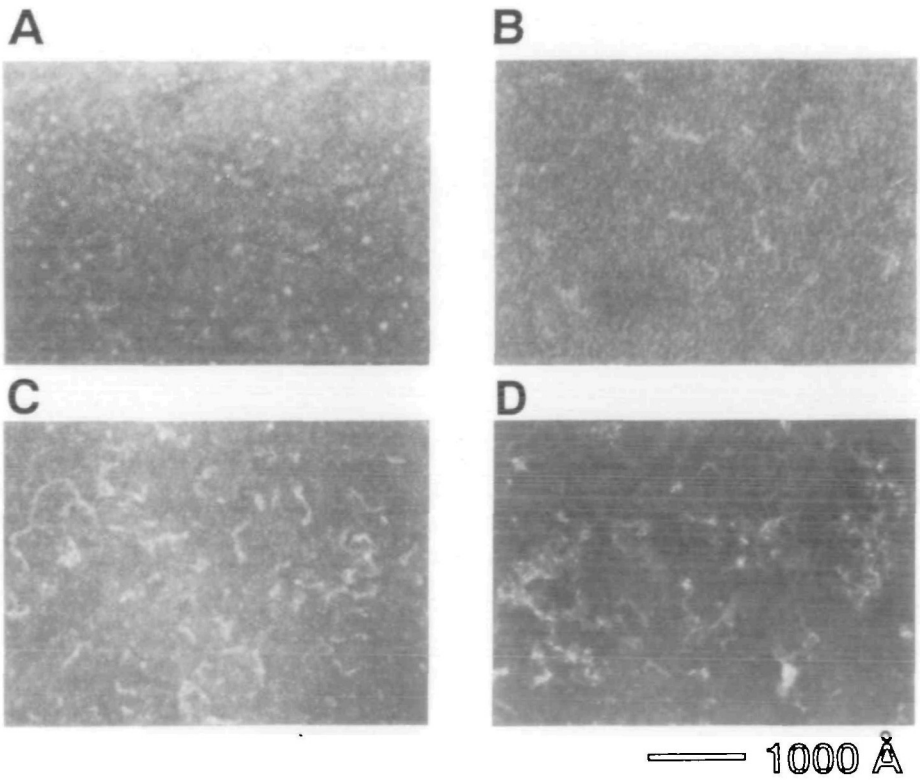

Fig. 2. **Transmission electron micrographs of ovalbumin aggregates.** The compactly misfolded ovalbumin was incubated at 2.8 mg/ml at 37°C for 5 h in the presence of 20 mM Hepes (pH 7.5) containing KCl at 0 mM (A), 50 mM (B), 150 mM (C), and 450 mM (D), respectively. The protein solutions were diluted with the same buffer used for preparing the specimen. The specimen was placed on a carbon-coated electron microscope grid, negatively stained with 2% potassium phosphotungstate, and observed with a transmission electron microscope operating at 100 kV. The magnification for photographs was ×40,000.

after incubation for 24 h showed the formation of large polymers of molecular size greater than 10^6 kDa (Fig. 1D). Aggregation became more pronounced as the concentration of salt added was increased, and prolonged incubation in the presence of 450 mM KCl generated aggregates too massive to pass through the gel matrix (data not shown). However, it should be noted that the peak remained unaltered at the position of a monomer, though it was decreased in height.

Shapes of Ovalbumin Aggregates—When the misfolded ovalbumin was incubated at 37°C for 5 h in the absence of KCl (Fig. 2A), oligomers were observed as very small particles. In the presence of 50 mM KCl (Fig. 2B), the molecules formed short, rod-like polymers. The addition of 150 mM KCl allowed the misfolded molecules to assemble into a long linear polymer (Fig. 2C). With the increase in the concentration of the salt, the linear polymers elongated and some could be observed intertwining. In the presence of 450 mM KCl, massive agglomerates were formed; the formation of ordered fibrous polymers was interrupted and a complex tangle of filaments was observed (Fig. 2D).

Effect of Different Anions on Polymerization of Ovalbumin—Salts with different species of anion induced the misfolded ovalbumin to precipitate at different concentrations. The concentrations of anions required to precipitate half of the misfolded ovalbumin were 0.9 M sulfate, 1 M phosphate, and 3.2 M acetate. Under the conditions we employed, chloride and iodide appeared to have no precipitating effect on the misfolded protein. However, a high concentration of chloride made the protein solution more viscous than did a similar concentration of iodide. Precipitation of the misfolded ovalbumin was progressively reduced in the following order of anions: sulfate, phosphate, acetate, chloride, and iodide.

An increase in light scattering reflects a change of the assembly of macromolecules in their size and shape. The TEM observation showed linear polymers of misfolded ovalbumin at the salt concentration of 150 mM, regardless of the species of anions. The order of effectiveness of anions in promoting the linear polymerization was shown to be sulfate > phosphate > acetate > fluoride > chloride > bromide > iodide > thiocyanate (Fig. 3).

Identification of Exposed Sulfhydryl Groups—We examined the behavior of cysteine residues as a consequence of defective folding of heat-denatured ovalbumin. None of the cysteine residues in the native ovalbumin was labeled with the fluorescent reagent, IAEDANS (data not shown). In contrast, six cysteine residues were labeled in the misfolded ovalbumin, albeit to varying extents (Fig. 4). The percentages of exposed cysteine residues were estimated to be 67.6, 68.4, 86.7, 82.7, 47.6, and 59.3% for Cys11, Cys30, Cys73, Cys120, Cys367, and Cys382, respectively. In the native protein, four cysteine residues (Cys11, Cys30, Cys367, and Cys382) are buried within a hydrophobic core that is sequestered from the solvent

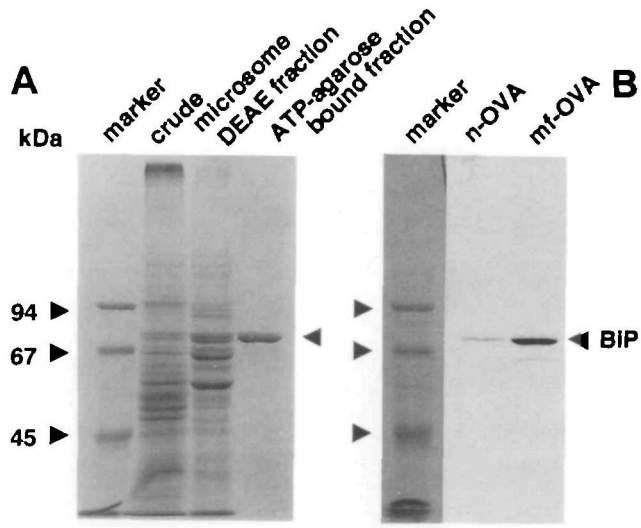

Fig. 5. **Purification of bovine BiP (A) and specific binding of bovine BiP to the misfolded ovalbumin (B).** (A) Microsomes were solubilized in Triton X-100 and passed over a DEAE Cellulofine column. The BiP-containing fraction was eluted with 200 mM NaCl, and the eluate was loaded onto an ATP-agarose column. BiP was eluted by addition of ATP. A 7.5% SDS-polyacrylamide gel stained with Coomassie Brilliant Blue shows the protein species present in aliquots of samples from different stages of the procedure for purification of bovine BiP. (B) Bovine BiP was incubated with either the native ovalbumin (n-OVA) or the misfolded protein (mf-OVA). The complexes were recovered with protein A Sepharose beads that had been precoated with anti-ovalbumin antibodies, analyzed by SDS-PAGE, and then transferred to a PVDF membrane. BiP was probed with rat monoclonal antibody to a peptide containing a heat shock conserved sequence.

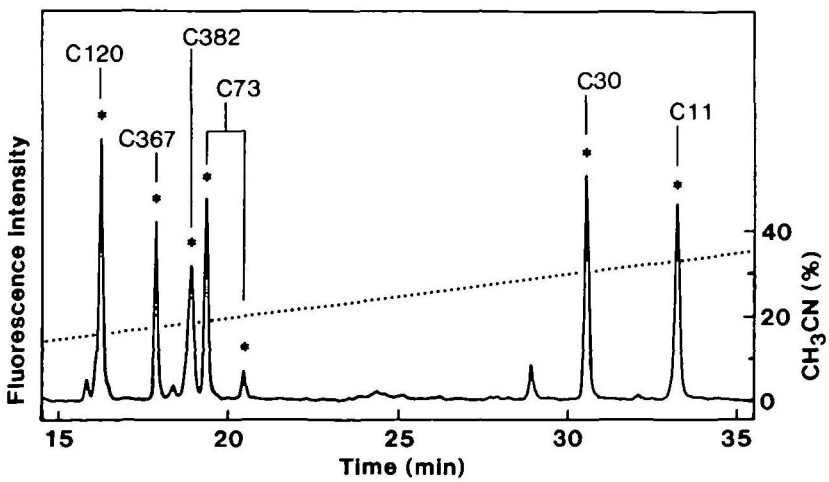

Fig. 4. **Elution profile of the peptides containing AEDANS-labeled cysteine residues.** The misfolded ovalbumin was labeled with IAEDANS, extensively digested with proteases, and fractionated by a reverse-phase HPLC column (4.6×150 mm; Cosmosil $5C_{18}$-AR) connected to an HPLC system (LC-10AS; Shimadzu) equipped with a spectrofluorometric detector (RF-550; Shimadzu). The seven peaks exhibiting AEDANS fluorescence (excitation, 340 nm; emission, 520 nm), which were identified as peptides containing labeled cysteine residues (C), are denoted by asterisks. The numbers following C show the positions of the cysteine residues in the primary structure of hen ovalbumin. The percentage of exposed cysteine residues was estimated from the ratio of areas of the peaks showing fluorescent material in a sample to those of the corresponding peaks in the standard.

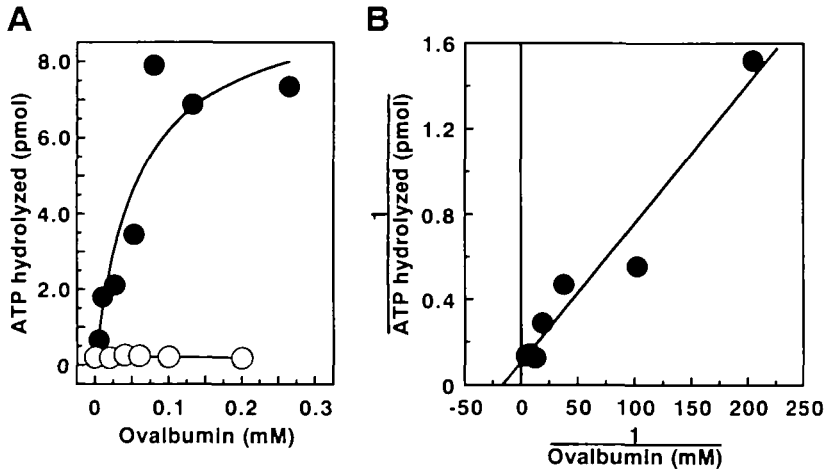

Fig. 6. **ATPase activity of bovine BiP stimulated by the misfolded ovalbumin.** Measurements of ATPase activity were done as described in "MATERIALS AND METHODS." (A) ATP hydrolysis by bovine BiP is a function of the concentration of the misfolded ovalbumin (closed circles) and the native protein (open circles). (B) Double reciprocal plot for the misfolded ovalbumin gives the kinetic parameters of K_m of 64 μM and V_{max} of 0.5 nmol/min per milligram for the ATPase activity of bovine BiP.

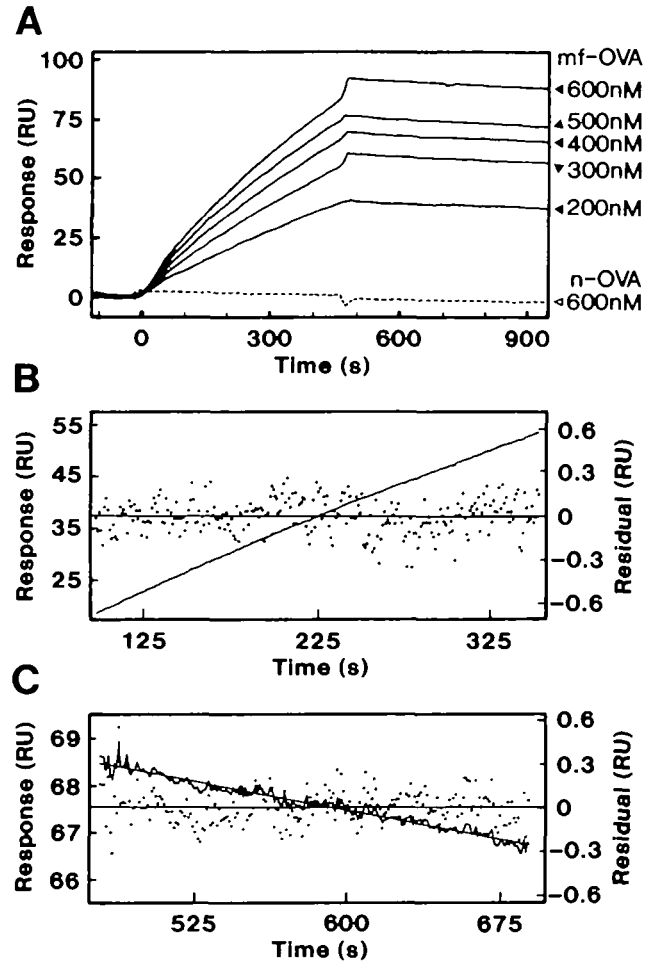

Fig. 7. **Surface plasmon resonance measurement of the interaction of the misfolded ovalbumin with the immobilized Fab fragment.** The immobilized ligand was the Fab fragment of a monoclonal antibody raised against radiochemically denatured ovalbumin. (A) Kinetic analysis of concentration-dependent binding to the immobilized Fab fragment of the misfolded ovalbumin. These curves gave a good fit to a two-component model of interaction. (B) and (C) are representative examples (400 nM) of the curve fitting and the residual plots of the association (χ^2=0.014) and dissociation (χ^2=0.013) phases, respectively.

TABLE I. **Kinetics for binding of the misfolded ovalbumin to the immobilized Fab fragment.** Measurements were done by using the BIAcore 2000™ system as described in "MATERIALS AND METHODS." Mean values ($\bar{X}$) of k_{ass}, k_{diss}, and K_d were determined for a series of Fab-ovalbumin samples using curve fitting to a simple two-component model of interaction (A+B=AB) for titration of the solution-phase ovalbumin, as for Fig. 7A. Numbers in brackets represent ± S.E. Analyses were done with BIAevaluation 2.0 software (Pharmacia). The equilibrium dissociation constant, K_d, was calculated from k_{diss}/k_{ass}.

Ovalbumin (nM)	k_{ass} ($M^{-1}\cdot s^{-1}$)	k_{diss} (s^{-1})	K_d (M)
200	3.55×10^{5}	1.12×10^{-4}	3.15×10^{-9}
300	3.15×10^{5}	1.10×10^{-4}	3.49×10^{-9}
400	2.68×10^{5}	1.21×10^{-4}	4.51×10^{-9}
500	2.65×10^{5}	1.29×10^{-4}	4.87×10^{-9}
600	2.26×10^{5}	1.04×10^{-4}	4.60×10^{-9}
$\bar{X}$ (±S.E.)	$2.86\ (\pm0.25)\times10^{5}$	$1.15\ (\pm0.05)\times10^{-4}$	$4.12\ (\pm0.38)\times10^{-9}$

molecules. In contrast, these results suggest that the cysteine residues are exposed to a solvent-accessible environment after a rapid cooling of heat-denatured ovalbumin. Another noteworthy feature was the occurrence of a thiol-disulfide exchange that led to the formation of various disulfide isomers, since both Cys73 and Cys120, which were originally disulfide-bonded, were labeled.

Interaction of Bovine BiP with Misfolded Ovalbumin—The two-step procedure with DEAE ion-exchange and ATP-agarose affinity chromatography yielded bovine BiP that was estimated to be 98% pure by densitometry following analysis by SDS-PAGE and staining with Coomassie Brilliant Blue (Fig. 5A). To determine whether purified BiP interacts with the misfolded ovalbumin, we incubated BiP with ovalbumin samples and then recovered BiP bound to ovalbumin with protein A Sepharose beads that had been precoated with anti-ovalbumin polyclonal antibody. Qualitative analysis from the immunoblotting revealed that the recovery was significantly higher when BiP reacted with the misfolded ovalbumin compared to the native protein (Fig. 5B). The faint band in the BiP binding to the native protein results from a direct interaction of BiP with antibody-coated Sepharose without the mediation of ovalbumin. Therefore, the difference in intensity between the two bands reflects the intrinsic binding of bovine BiP to the

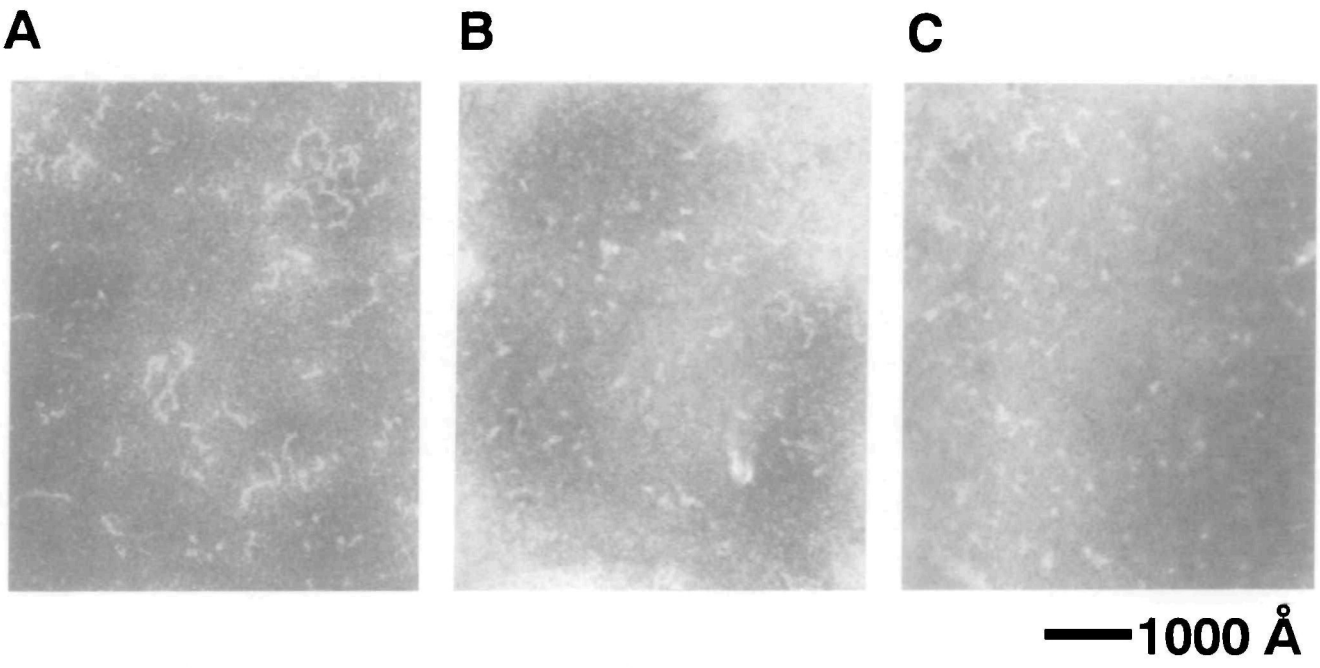

Fig. 8. **Transmission electron micrographs showing the inhibition of formation of ovalbumin polymers.** Polymerization was conducted in the absence of a competitor (A) and in the presence of either bovine BiP (B) or the Fab fragment of monoclonal antibody raised against radiochemically denatured ovalbumin (C). The magnification for photographs was ×40,000.

misfolded ovalbumin molecules.

Binding specificity of bovine BiP was also confirmed by the stimulation of polypeptide-dependent ATPase activity (Fig. 6A). The native ovalbumin did not display any ATPase-stimulatory activity. In contrast, the initial rate of ATP hydrolysis by BiP was dependent on the concentration of the misfolded ovalbumin. The misfolded protein elicited the ATPase activity of bovine BiP, having the K_m for ATP hydrolysis of 64 μM. The kinetic data gave a linear double-reciprocal plot yielding the V_{max} of 0.5 nmol/min per milligram for bovine BiP driven by the misfolded ovalbumin (Fig. 6B).

Binding of Fab Fragment to Misfolded Ovalbumin—As a ligand immobilized on the dextran matrix, we used the Fab fragment of monoclonal antibody raised against radiochemically denatured ovalbumin. Panel A in Fig. 7 shows the titration of binding of the misfolded ovalbumin to the immobilized Fab fragment. Injection of the native ovalbumin did not result in a rise in the sensorgram. In contrast, a significant rise in the sensorgram was observed in a concentration-dependent manner for the misfolded ovalbumin. Curve-fitting analysis of the binding phase of these curves gave an estimated association rate constant k_{ass} of 2.86×10^3 $M^{-1}\cdot s^{-1}$ (Fig. 7B) and a dissociation rate constant k_{diss} of 1.15×10^{-4} s^{-1} (Fig. 7C). These calculated values suggested that the misfolded ovalbumin associated slowly with and bound ovalbumin dissociated slowly from the immobilized Fab fragment. The equilibrium dissociation constant K_d was calculated to be 4.12×10^{-8} M (Table I). These results indicated that the Fab fragment bound specifically to the misfolded ovalbumin with high affinity, but not to the native protein.

Inhibition of Elongation of Ovalbumin Polymer—We examined the inhibitory effects of bovine BiP and the anti-ovalbumin Fab fragment on the formation of ovalbumin polymers catalyzed by KCl. The absence of a competitor allowed the misfolded protein to assemble progressively in a linear fashion (Fig. 8A). However, the polymerization was significantly suppressed by addition of bovine BiP (Fig. 8B). The anti-ovalbumin Fab fragment markedly inhibited linear polymerization of the misfolded molecules (Fig. 8C). The Fab fragment of monoclonal antibody raised against transglutaminase, native ovalbumin and BSA did not display any inhibitory effect on the elongation of the polymer chain (data not shown).

DISCUSSION

The results of size-exclusion chromatography (Fig. 1) suggested that the misfolded ovalbumin, which was obtained by cooling heat-denatured protein rapidly, partitions between two fates, non-specific aggregation and productive renaturation. This partitioning depends critically on the concentration of salt added. As the salt concentration was increased, aggregation developed progressively and the assembly geometry of the misfolded ovalbumin changed from a linear polymer into a massive agglomerate (Fig. 2).

The polymerization depended on the species of anion employed. The order of effectiveness of anions in promoting the linear polymerization was shown to be sulfate > phosphate > acetate > fluoride > chloride > bromide > iodide > thiocyanate (Fig. 3). This order follows the lyotropic series first demonstrated by Hofmeister for the salting-out of euglobulins (*36*). Protein conformation can be perturbed by the addition of salts, which influence the electrostatic interactions of charged groups and polar groups, and affect hydrophobic interaction *via* modification of the water structure (*37, 38*). The degree to which water structure is affected depends on the nature of the anions and follows the lyotropic series (*39*). Stabilizing anions such as

sulfate and phosphate increase the surface tension of water and cause preferential hydration of a protein, which leads to a more favorable energetic state by the sequestering of nonpolar groups from solvent molecules, thereby enhancing hydrophobic interaction. In contrast, destabilizing anions such as iodide and thiocyanate reduce the energy required to transfer the nonpolar groups into water, thereby weakening hydrophobic interaction (*37, 39*). Therefore, the effects of anions in the linear polymerization support the view that denatured protein molecules aggregate through hydrophobic interaction.

Care is needed in interpreting the effect of anions on linear polymerization (*40*), because the Hofmeister series pertains to salts at high concentrations. The salt concentration required for linear polymerization of the misfolded ovalbumin could be evaluated as a marginal concentration to exhibit the preferential effect of anions on protein assembly. The effect of anions may be amplified as a result of increased hydrophobicity in the misfolded ovalbumin compared with the native protein. Indeed, when the surface hydrophobicity was compared between the misfolded ovalbumin and the native protein, the former exhibited significant fluorescence of a chromophore, ANS, whereas the latter did not display any fluorescence (Tani, F. *et al.*, submitted for publication). Moreover, the misfolded ovalbumin contained exposed cysteine residues in hydrophobic sequences that are normally located in the interior of the native protein (Figs. 4 and 9).

The involvement of hydrophobic interaction in linear polymerization was confirmed by the finding that the linear polymerization was inhibited by intrinsic binding of bovine BiP to the misfolded ovalbumin (Fig. 8B). Mammalian BiP has the ability to bind to a variety of peptide sequences with a broad spectrum of hydrophobicity in an ATP-dependent manner (*30, 41, 42*). The K_m of various synthetic peptides for the ATPase activity of bovine BiP varies from 10 μM to >1 mM (*30, 42*). Flynn *et al.* determined the V_{max} of bovine BiP driven by the peptides to be approximately 1.0 to 2.0 nmol/min per milligram (*30*). Bovine BiP bound to the misfolded ovalbumin, but not to the native protein, in an ATP-dependent manner (Figs. 5 and 6). The K_m and V_{max} values we estimated were similar in magnitude to those reported before. This specific binding reflects a typical characteristic of the interaction of the molecular chaperone BiP with a denatured protein, although the equilibrium dissociation constant remains to be determined. It thus follows that the compactly misfolded ovalbumin polymerized through hydrophobic interaction occurring among the areas exposed as a result of the defective folding of the heat-denatured protein.

A sequence-specific Fab fragment of the monoclonal antibody, which was raised against radiochemically denatured ovalbumin, enabled us to probe a possible interaction site among the misfolded molecules owing to the high specificity of its complementarity determining region. The epitopes that are exposed on a denatured protein but occluded in its polymer are possible interaction sites. Therefore, the epitope of a sequence-specific antibody that retards the linear polymerization of misfolded ovalbumin molecules can be identified as a candidate interaction site. The Fab fragment we employed was highly conformation-sensitive with specific binding to misfolded ovalbumin, but with no reactivity to the native protein (Fig. 7), and it had a low dissociation constant K_d of 4.12×10^{-8} M to the misfolded protein (Table I). Since the Fab fragment, of which the epitope included the sequence from residues 172 to 183 [^{172}MVLVNAIVFKGL^{183}] in the primary structure of hen ovalbumin (Fig. 9), inhibited the linear polymerization of the misfolded ovalbumin (Fig. 8C), the simplest interpretation of our result is that the sequence from residues 172 to 183 is part of, or close to, one of the regions of axial contact among the misfolded ovalbumin molecules. The presence of many aliphatic amino acid residues in the epitope sequence is evidence in favor of hydrophobic interaction as a factor in the polymerization. However, we cannot exclude the possibility of other segments as interac-

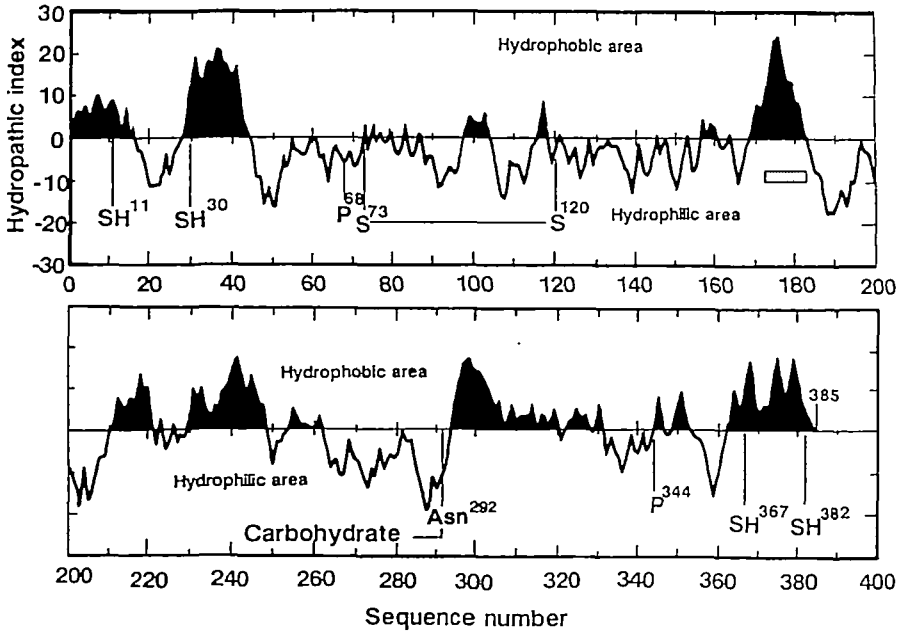

Fig. 9. **Hydropathy profile of the primary structure of native ovalbumin.** The hydropathy profile of ovalbumin was depicted by plotting the averaged hydropathy index (*46*) of a nonapeptide composed of amino acid residues $i-4$ to $i+4$ versus i, the residue number of the amino acid. The computer program SDC-GENETYX (Software Developing, Tokyo) was used for this analysis. The primary structure of ovalbumin reported by Nisbet *et al.* (*47*) was employed. Hydrophobic regions are drawn black and the epitope of the monoclonal Fab fragment we employed is delineated by the dotted bar. Free sulfhydryl groups of cysteine residues in the native protein are represented as SH with numbers that show their positions in the primary structure. An original disulfide bond (S-S) links Cys73 and Cys120.

tion sites because the hydropathy index of hen ovalbumin shows the presence of seven hydrophobic sequences in the primary structure (Fig. 9).

The mechanism of polymerization caused by defective folding of heat-denatured ovalbumin can be explained by reference to the model of loop-sheet polymerization of the Z type variant of α_1-antitrypsin. It seems likely that the molecular structure of the active serpin α_1-antitrypsin corresponds to that of native ovalbumin. In the α_1-antitrypsin cleaved at the reactive-center loop, the amino-terminal segment of the loop is incorporated in the gap between β-strands 3A and 5A (*43*). The separate peptide corresponding to the incorporated segment prevented spontaneous polymerization of the Z variant (*15, 17*). In the proposed model, in which the mobile reactive-center loop of one molecule is inserted into the central β-sheet A of another (*15–18*), an opening of β-sheet A is required for the insertion of the loop. It is noteworthy that the peptide segment of residues 172 to 183 recognized by the Fab fragment is a part of the central β-strand 3A of hen ovalbumin (Fig. 10A). The β-strand 3A is packed intramolecularly under the cover of helix F in the native ovalbumin. The binding of the Fab fragment to the misfolded ovalbumin (Fig. 7) clearly indicates that the structure of, or around, β-sheet A was misconstructed, with the exposure of β-strand 3A, during the refolding process of heat-denatured ovalbumin. The presence of a non-native structure of β-sheet A was supported by the labeling of Cys30 (Fig. 4). The "shutter domain" (Fig. 10B) is a functional domain for maintenance of the correct architecture of β-sheet A (*4*). Perturbation of the shutter domain facilitates the polymerization of two α_1-antitrypsin variants (*44, 45*). This domain is located beneath the β-strand 3A and corresponds to the Tyr-Cys-Pro [29–31] sequence at the commencement of helix B in the native ovalbumin. The labeling of Cys30 in the misfolded ovalbumin indicates a non-native structure of the shutter domain and implies an insufficient organization of the

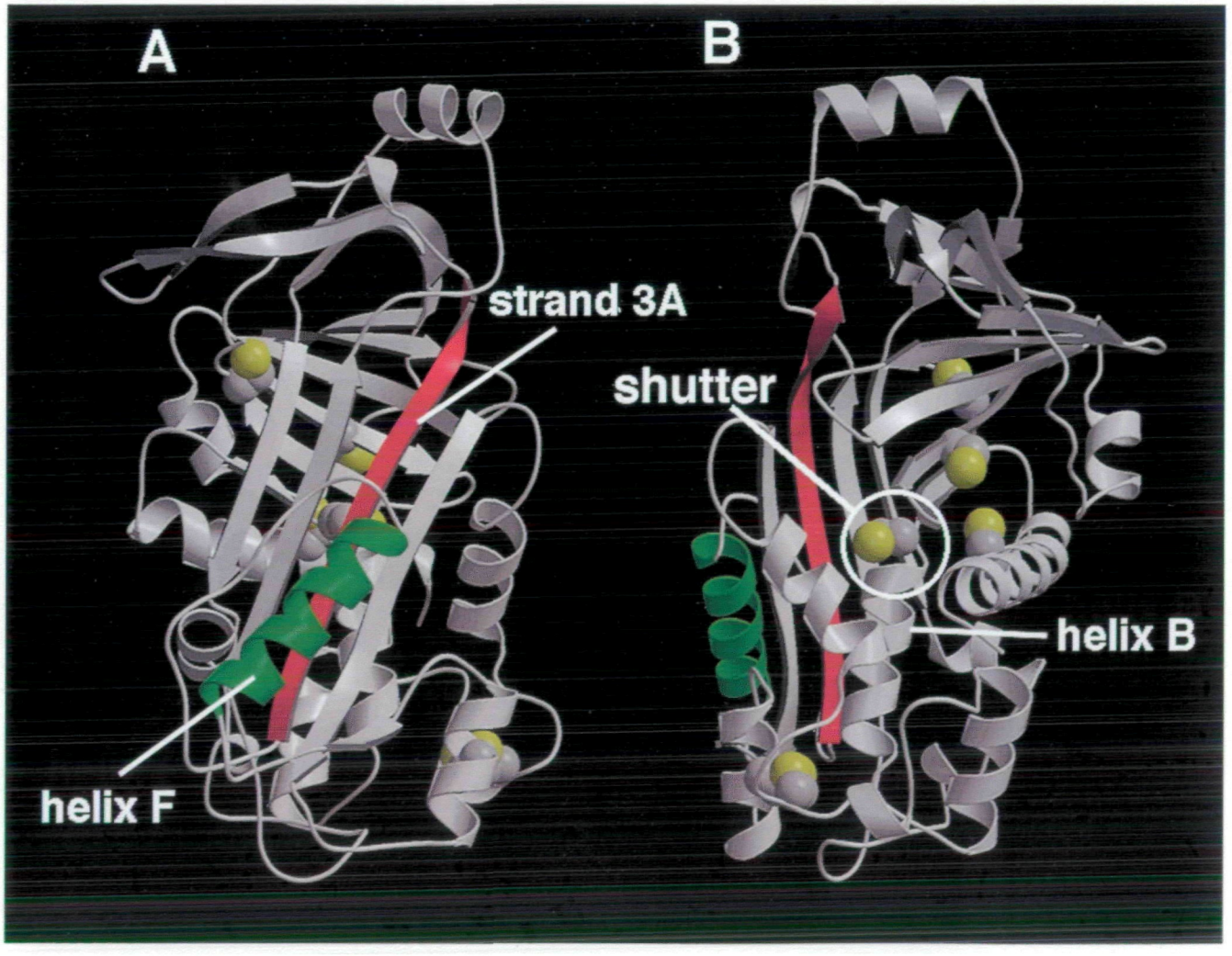

Fig. 10. **Schematic representation of the structure of native ovalbumin (*23*).** α-Helices are represented by ribbons and strands of β-sheets by arrows. Sulfur atoms, and both α- and β-carbon atoms in cysteine residues are shown as yellow and gray spheres, respectively. (A) The β-strand 3A containing the epitope of the Fab fragment is represented by red and α-helix F is represented by green. The epitope is packed intramolecularly under the cover of helix F in the native ovalbumin. (B) The shutter domain beneath the β-strand 3A is circled. The domain is located beneath the β-strand 3A and corresponds to the Tyr-Cys-Pro [29–31] sequence at the commencement of helix B in the native ovalbumin. The diagram was drawn using the programs MOLSCRIPT (*48*) and Raster3D Ver. 2.0 (*49*).

central β-sheet A. Therefore, we conclude that exposure of the region of, or adjacent to, β-strand 3A in the central sheet A is required for hydrophobic contact among the misfolded ovalbumin molecules.

Analysis of disulfide pairing revealed that the misfolded ovalbumin molecules were composed of a variety of disulfide isomers (Tani, F. *et al.*, submitted for publication). For this reason, it remains unclear whether the polymerization can be mediated by either a few definite and sequence-specific regions or multiple and non-specific hydrophobic regions. However, it seems likely that the disulfide isomers resemble each other, in that a large portion of the misfolded molecules formed dimers with the Fab fragment, regardless of differences in local structures. Therefore, we consider that a common feature in the defective folding of heat-denatured ovalbumin is exposure of the hydrophobic region of β-sheet A.

In conclusion, rapid folding of heat-denatured ovalbumin caused a lack of organization of, or adjacent to, the central β-sheet A, thereby leading to the exposure of hydrophobic regions in the compactly misfolded ovalbumin. The preferential effect of anions and the inhibitory effect of BiP indicated that the compactly misfolded ovalbumin polymerized through hydrophobic interaction. A sequence-specific antibody revealed that a possible interaction site for axial contact among the misfolded molecules is a segment of β-strand 3A. This polymerization process may be explained by reference to the mechanism postulated for loop-sheet polymerization in the Z type variant of a serpin α_1-antitrypsin. Together with some genetic variants of serpins, ovalbumin, a non-inhibitory serpin, seems likely to serve as a promising model for elucidating the kinetic mechanism of serpin folding.

The authors thank Dr. K. Ikura (Kyoto Institute of Technology) for providing the monoclonal antibody raised against transglutaminase.

REFERENCES

1. Kim, P.S. and Baldwin, R.L. (1990) Intermediates in the folding reactions of small proteins. *Annu. Rev. Biochem.* **59**, 631-660
2. Matthews, C.R. (1993) Pathways of protein folding. *Annu. Rev. Biochem.* **62**, 653-683
3. Dobson, C.M. (1995) Finding the right fold. *Nature Struct. Biol.* **2**, 513-517
4. Stein, P.E. and Carrell, R.W. (1995) What do dysfunctional serpins tell us about molecular mobility and disease? *Nature Struct. Biol.* **2**, 96-113
5. Travis, J. and Salvesen, G.S. (1983) Human plasma proteinase inhibitors. *Annu. Rev. Biochem.* **52**, 655-709
6. Sifers, R.N., Carlson, J.A., Clift, S.M., Demayo, F.J., Bullock, D.W., and Woo, S.L.C. (1987) Tissue specific expression of the human alpha-1-antitrypsin gene in transgenic mice. *Nucleic Acids Res.* **15**, 1459-1475
7. Gadek, J.E., Fells, G.A., Zimmerman, R.L., Rennard, S.I., and Crystal, R.G. (1981) Antielastases of the human alveolar structures: Implications for the protease-antiprotease theory of emphysema. *J. Clin. Invest.* **68**, 889-898
8. Laurell, C.B. and Eriksson, S. (1963) The electrophoretic α_1-globulin pattern of serum in α_1-antitrypsin deficiency. *Scand. J. Clin. Lab. Invest.* **15**, 132-140
9. Jeppsson, J.-O. (1976) Amino acid substitution Glu→Lys in α_1-antitrypsin PiZ. *FEBS Lett.* **65**, 195-197
10. Brantly, M., Nukiwa, Y., and Crystal, R.G. (1988) Molecular basis of alpha-1-antitrypsin deficiency. *Am. J. Med.* **84**, 13-31
11. Crystal, R.G. (1989) The α_1-antitrypsin gene and its deficiency states. *Trends Genet.* **5**, 411-417
12. Sifers, R.N., Finegold, M.J., and Woo, S.L.C. (1989) Alpha-1-antitrypsin deficiency: Accumulation or degradation of mutant variants within the hepatic endoplasmic reticulum. *Am. J. Respir. Cell Mol. Biol.* **1**, 341-345
13. Yu, M.-H., Lee, K.N., and Kim, J. (1995) The Z type variation of human α_1-antitrypsin causes a protein folding defect. *Nature Struct. Biol.* **2**, 363-367
14. Sifers, R.N. (1995) Defective protein folding as a cause of disease. *Nature Struct. Biol.* **2**, 355-357
15. Lomas, D.A., Evans, D.L., Finch, J.T., and Carrell, R.W. (1992) The mechanism of Z α_1-antitrypsin accumulation in the liver. *Nature* **357**, 605-607
16. Sifers, R.N. (1992) Protein transport. Z and the insoluble answer. *Nature* **357**, 541-542
17. Mast, A.E., Enghild, J.J., and Sawesen, G. (1992) Conformation of the reactive site loop at α_1-proteinase inhibitor probed by limited proteolysis. *Biochemistry* **31**, 2720-2728
18. Lomas, D.A., Evans, D.L., Stone, S.R., Chang, W.-S.W., and Carrell, R.W. (1993) Effect of the Z mutation on the physical and inhibitory properties of α_1-antitrypsin. *Biochemistry* **32**, 500-508
19. Huber, R. and Carrell, R.W. (1989) Implications of three-dimensional structure of α_1-antitrypsin for structure and function of serpins. *Biochemistry* **28**, 8951-8966
20. Long, W.F. and Williamson, F.B. (1980) Ovalbumin, a protein possessing sequence homologies with antithrombin III and α_1-antitrypsin, lacks anti-thrombin and anti-Xa activities. *I.R.C.S. Med. Sci.* **8**, 808
21. Ødum, L. (1987) Trypsin-inhibitory activity of ovalbumin preparations is due to ovomucoid. *Biol. Chem. Hoppe-Seyler* **368**, 1603-1606
22. Wright, H.T. (1984) Ovalbumin is an elastase substrate. *J. Biol. Chem.* **259**, 14335-14336
23. Stein, P.E., Leslie, A.G., Finch, J.T., and Carrell, R.W. (1991) Crystal structure of uncleaved ovalbumin at 1.95 Å resolution. *J. Mol. Biol.* **221**, 941-959
24. Tatsumi, E., Takahashi, N., and Hirose, M. (1994) Denatured state of ovalbumin in high concentrations of urea as evaluated by disulfide rearrangement analysis. *J. Biol. Chem.* **269**, 28062-28067
25. Takahashi, N. and Hirose, M. (1992) Reversible denaturation of disulfide-reduced ovalbumin and its reoxidation generating the native cystine cross-link. *J. Biol. Chem.* **267**, 11565-11572
26. Koseki, T., Kitabatake, N., and Doi, E. (1989) Irreversible thermal denaturation and formation of linear aggregates of ovalbumin. *Food Hydrocolloids* **3**, 123-134
27. Tani, F., Murata, M., Higasa, T., Goto, M., Kitabatake, N., and Doi, E. (1995) Molten globule state of protein molecules in heat-induced transparent food gels. *J. Agric. Food Chem.* **43**, 2325-2331
28. Sörensen, S.P.L. and Höyrup, M. (1915) Studies on proteins. I. On the preparation of egg-albumin solutions of well-defined composition, and on the analytical methods used. *Compt. Rend. Trav. Lab. Carlsberg* **12**, 12-67
29. Kurtz, S., Rossi, J., Petko, L., and Lindquist, S. (1986) An ancient developmental induction: Heat shock proteins induced in sporulation and oogenesis. *Science* **231**, 1154-1157
30. Flynn, G.C., Chappell, T.G., and Rothman, J.E. (1989) Peptide binding and release by proteins implicated as catalysts of protein assembly. *Science* **245**, 385-390
31. Laemmli, U.K. (1970) Cleavage of structural proteins during the assembly of the head of bacteriophage T4. *Nature* **227**, 680-685
32. Hirano, H. (1989) Microsequence analysis of winged bean seed proteins electroblotted from two-dimensional gel. *J. Protein Chem.* **8**, 115-130
33. Shlomai, J. and Kornberg, A. (1980) A prepriming DNA replication enzyme of *Escherichia coli*. I. Purification of protein n′: a sequence-specific, DNA-dependent ATPase. *J. Biol. Chem.* **255**, 6789-6793
34. Jönsson, U., Fägerstam, L., Ivarsson, B., Johnsson, B., Karlsson, R., Lundh, K., Löfås, S., Persson, B., Roos, H., Rönnberg, I., Sjölander, S., Stenberg, E., Ståhlberg, R., Urbaniczky, C.,

Östlin, H., and Malmqvist, M. (1991) Real-time biospecific interaction analysis using surface plasmon resonance and sensor chip technology. *BioTechniques* **11**, 620-627
35. Johnsson, B., Löfås, S., and Lindquist, G. (1991) Immobilization of proteins to a carboxymethyldextran-modified gold surface for biospecific interaction analysis in surface plasmon resonance sensors. *Anal. Biochem.* **198**, 268-277
36. Hofmeister, F. (1888) Zur lehre von der wirkung der salze. Zweite mittheilung. *Arch. Exptl. Pathol. Pharmakol.* **24**, 247-260
37. von Hippel, P.H. and Schleich, T. (1969) Ion effects on the solution structure of biological macromolecules. *Acc. Chem. Res.* **2**, 257-265
38. Hatefi, Y. and Hanstein, W.G. (1969) Solubilization of particulate proteins and nonelectrolytes by chaotropic agents. *Proc. Natl. Acad. Sci. USA* **62**, 1129-1136
39. von Hippel, P.H. and Wong, K.Y. (1965) On the conformational stability of globular proteins: The effects of various electrolytes and nonelectrolytes on the thermal ribonuclease transition. *J. Biol. Chem.* **240**, 3909-3923
40. Leberman, R. (1991) The Hofmeister series and ionic strength. *FEBS Lett.* **284**, 293-294
41. Flynn, G.C., Pohl, J., Flocco, M.T., and Rothman, J.E. (1991) Peptide-binding specificity of the molecular chaperone BiP. *Nature* **353**, 726-730
42. Blond-Elguindi, S., Cwirla, S.E., Dower, W.J., Lipshutz, R.J., Sprang, S.R., Sambrook, J., and Gething, M.-J.H. (1993) Affinity panning of a library of peptides displayed on bacteriophages reveals the binding specificity of BiP. *Cell* **75**, 717-728
43. Loebermann, H., Tokuoka, R., Deisenhofer, J., and Huber, R. (1984) Human α_1-proteinase inhibitor: crystal structure analysis of two crystal modifications, molecular model and preliminary analysis of the implications for function. *J. Mol. Biol.* **177**, 531-556
44. Frazier, G.C., Harrold, T.R., Hofker, M.H., and Cox, D.W. (1989) In-frame single codon deletion in the M malton deficiency allele of α_1-antitrypsin. *Am. J. Hum. Genet.* **44**, 894-902
45. Seyama, K., Nukiwa, T., Takabe, K., Takahashi, H., Miyake, K., and Kira, S. (1991) S_{Iiyama} (serine 53 (TCC) to phenylalanine 53 (TTC)): A new α_1-antitrypsin-deficient variant with mutation on a predicted conserved residue of the serpin backbone. *J. Biol. Chem.* **266**, 12627-12632
46. Kyte, J. and Doolittle, R.F. (1982) A simple method for displaying the hydropathic character of a protein. *J. Mol. Biol.* **157**, 105-132
47. Nisbet, A.D., Saundry, R.H., Moir, A.J.G., Fothergill, L.A., and Fothergill, J.E. (1981) The complete amino-acid sequence of hen ovalbumin. *Eur. J. Biochem.* **115**, 335-345
48. Kraulis, P. (1991) MOLSCRIPT: a program to produce both detailed and schematic plots of protein structures. *J. Appl. Crystallog.* **24**, 946-950
49. Merritt, E.A. and Murphy, E.P. (1994) Raster3D version 2.0. A program for photorealistic molecular graphics. *Acta. Crystallog. sect. D* **50**, 869-873